PROCEEDINGS OF SPIE

SPIEDigitalLibrary.org/conference-proceedings-of-spie

The reformatting advantage: photonics vs. conventional optics!

Ariadna Calcines, Robert Harris, Roger Haynes, Dionne Haynes

Ariadna Calcines, Robert J. Harris, Roger Haynes, Dionne Haynes, "The reformatting advantage: photonics vs. conventional optics!," Proc. SPIE 10706, Advances in Optical and Mechanical Technologies for Telescopes and Instrumentation III, 107062G (10 July 2018); doi: 10.1117/12.2312110

SPIE.

Event: SPIE Astronomical Telescopes + Instrumentation, 2018, Austin, Texas, United States

Downloaded From: https://www.spiedigitallibrary.org/conference-proceedings-of-spie on 17 Jan 2023 Terms of Use: https://www.spiedigitallibrary.org/terms-of-use

The reformatting advantage - Photonics vs conventional optics!

Ariadna Calcines[a], Robert J. Harris[b], Roger Haynes[c], and Dionne Haynes[c]

[a]Centre for Advanced Instrumentation, Durham University, South Road DH1 3LE, Durham, United Kingdom
[b]Zentrum für Astronomie der Universität Heidelberg, Landessternwarte Königstuhl, Königstuhl 12, 69117 Heidelberg
[c]Leibniz-Institut für Astrophysik Potsdam, An der Sternwarte 16, D-14482 Potsdam, Germany

ABSTRACT

In recent decades, spectroscopic capabilities have been significantly enhanced by new technological developments, in particular spatial reformatting. Spatial reformatting allows multiple functionalities: the observation of a larger area of sky, obtaining the spectra of all spatial elements under the same atmospheric conditions; modification of the shape and size of the field of view; focal-ratio conversion for the optimized coupling between the telescope and the spectrograph; increase in the spatial and spectral resolving power; the observation of multiple objects; homogeneity in the illumination; scrambling of spatial and/or phase induced structure with the instrument, thus improving the system stability; relocation of the exit pupil, especially important for telecentric systems. The impact of reformatting and the breadth of science cases is so great that many alternative methods and technologies have been proposed: image slicers using refractive or reflective solutions; optical fibers with different core sizes and geometries; microlenses used in isolation or combined with fibers and more recently, photonic devices such as Photonic lanterns to produce modal decomposition. In this paper, a comparison between all currently available options is presented, with a detailed analysis of their advantages and limitations and a proposal for a new reformatter combining slicers and photonic devices. This proposal presents the advantages of the other alternatives and additionally offers: minimization of focal-ratio degradation; produces image and modal decomposition; improves the throughput along the spectral range, increases the spectral resolving power and adds the functionality of scrambling. All of these advantages are combined in a system where photonic and astronomical instrumentation capabilities are joined in an innovative solution with many applications, like for example, the Extremely Large Telescope.

Keywords: Photonic lanterns, image slicers, optical fibers, reformatting, Integral Field Unit, Astrophotonics, Integral Field Spectroscopy.

1. INTRODUCTION TO REFORMATTING AND INTEGRAL FIELD SPECTROSCOPY

Spectroscopy is one of the most powerful techniques in astronomy as it provides information about the object's flux at each wavelength. This allows astronomers to perform analysis not possible with imaging: kinematic and composition studies and detection of exoplanets to name a few. This important technique has been enhanced in the last few decades by technological developments, one of the most relevant ones is spatial reformatting.

Some decades ago standard spectrographs used an entrance slit to limit the field of view (FoV). For those science cases in which a larger area of the sky had to be observed, the image at the telescope focal plane (slit position) was displaced across the slit length using a scanning system.[1] This allowed the instrument to cover a significantly larger FoV by obtaining the spectra of adjacent fields in sequential observations and organizing

Further author information: (Send correspondence to A.C.)
A.C.: E-mail: ariadna.calcines@durham.ac.uk, Telephone: +44 (0) 191 334 3908

Advances in Optical and Mechanical Technologies for Telescopes and Instrumentation III, edited by Ramón Navarro, Roland Geyl, Proc. of SPIE Vol. 10706, 107062G · © 2018 SPIE
CCC code: 0277-786X/18/$18 · doi: 10.1117/12.2312110

Downloaded From: https://www.spiedigitallibrary.org/conference-proceedings-of-spie on 17 Jan 2023
Terms of Use: https://www.spiedigitallibrary.org/terms-of-use

them as a mosaic.[2] Although this improvement allowed an increase of the observed area of the sky, it could not avoid the rapid changes of the atmosphere and, as a consequence, every piece of the mosaic was obtained under different atmospheric conditions losing spatial continuity and increasing the difficulty when comparing the results. With the goal of increasing the FoV in a single exposure, different ideas to decompose the FoV and then reformat it into one or more slits were proposed. This led to the idea of enhancing the conventional spectroscopy towards integral field spectroscopy (IFS).

IFS allows the astronomer to obtain a datacube with spatial information along two axes (X, Y) and the spectrum of all sampling elements (λ). The optical systems used for this purpose are called integral field units (IFUs). IFUs were initially used to increase the FoV and reformat it into different geometries, such as a long slit or several separate slits feeding a spectrograph. More recently, numerous developments have occurred in this field leading to systems that can: reorganize a bi-dimensional FoV to feed a spectrograph; produce magnification (ordinary or anamorphic); modify the focal-ratio for the optimized coupling between telescope and instrument; define the appropriate sampling; transport the light from the telescope focus to the spectrograph and increase the spectral resolving power.

With the development of larger telescopes and the requirements of ultra-stable high resolution spectrographs new solutions are required. This is because, for a given set of performance parameters (e.g. spectral resolving power, image scale, adaptive optics (AO) corrected image quality, number of waveguide modes in the optical fiber system), the larger size of the primary mirror for the ELT class telescopes require a corresponding increase in the size, mass, complexity and cost of the instrumentation. An alternative is for the instrument FoV or the telescope-pupil to be sub-divided in units that can be processed separately, leading to manageable modular systems. Such modularity has already been adopted on the 8-10 m class telescope with instruments such as MUSE and VIRUS that have enabled unprecedented FoV and spectral coverage combination.

We call our proposed solution photonic slicer, a combination of slicers and photonic technologies. This combination facilitates the advantages offered by both technologies, e.g. the efficient and achromatic image slicing provided by mirror based slicers along with the filtering, flexible spatial re-formatting and increased optical stability provided by optical fibers and photonic devices.

In this paper, an overview of the different methods used for reformatting is presented in Section 2, followed by a description of the available reformatting technologies in Section 3. In Section 4 we describe three different conditions for astronomical observation: natural seeing; partial AO correction and diffraction limited. Our proposal for a reformatting alternative, combining "conventional" mirror based slicers and photonic devices is presented in Section 5. A summary of this research is presented in Section 6 where the advantages of our system are highlighted.

2. REFORMATTING AND SLICING PRINCIPLES

Reformatting and slicing provides a mechanism to reconfigure an optical system into a more convenient geometry. This allows, for example: the reduction of the effective slit width, increasing the spectral resolving power for a given spectrograph design; the division of an image into spatially separate components, allowing one to spectrally map different regions of an extended source using IFS; division of the pupil image to generate smaller apertures to modularize instrumentation or for wavefront sensing; mode separation for modularization, spatial filtering and/or photonic functionality. In each case above the reformatting and slicing enable a reduction in the size and complexity of the instrument components and adds functionality. Each principle is addressed in more detail below.

2.1 Field splitting

Field splitting is a technique that enables the FoV to be divided into smaller, more manageable parts, e.g. when the FoV is distributed to more than one spectrograph[3] or when several slits in one spectrograph are required. With mirror based splitters, the field is usually divided along one spatial direction (i.e. sliced) into as many sub-fields as the number of generated slits and an IFU for each sub-field is required. The idea of combining the field splitter and the slicer mirror array of an image slicer IFU has been proposed for the European Solar Telescope.[4] With a fiber based splitter the FoV would be divided along two spatial axes (i.e. diced) and then reconfigured into linear arrays (i.e. a slit or series of slits).

Downloaded From: https://www.spiedigitallibrary.org/conference-proceedings-of-spie on 17 Jan 2023
Terms of Use: https://www.spiedigitallibrary.org/terms-of-use

2.2 Image slicing

Image slicing essentially consists in dividing the image generated by the telescope into slices, where the shape and size can be arbitrary, however, typically the FoV is linearly sliced into thin rectangular pieces or diced into square (or hexagonal for microlenses or fiber based technologies) pieces. Image slicing can be usefully applied to different types of instrumentation, not only spectrographs. Slicing is typically performed at the telescope image focal plane, however, it can also be implemented at the instrument image focal plane (output slicing) to distribute the image to several detectors. Unlike field splitting, with image slicing it is important that the separate spatial information of the original FoV is retained, so the original 2D image can be reconstructed in software. For typical IFU instruments such a reconstructed image is referred to as a data-cube and contains the 2D spatial information as well as the associated spectral information.

In IFU systems the width of the slicer element defines the sampling and usually the slit width, however this can be adjusted with magnification. The slice width is related to spatial sampling and a defining parameter with regards the system spectral and spatial resolution. When the image is diced instead of sliced, the same image slicing concept can be found under the name of image dicing (see Fig. 1).

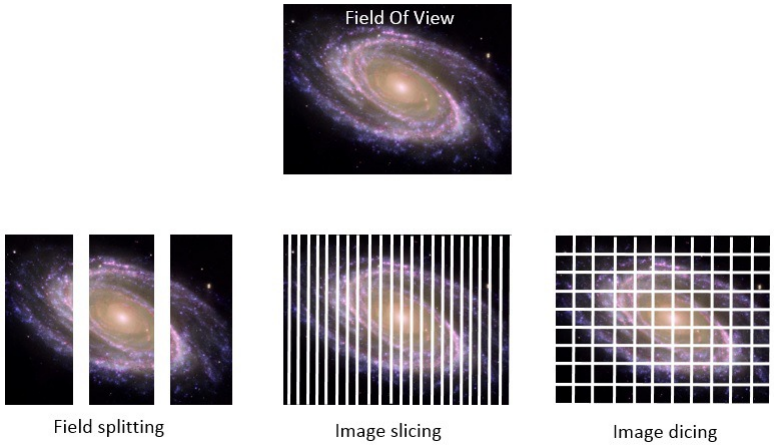

Figure 1. Differences between field splitting, image slicing and dicing. Field splitting divides the field of view (FoV) into sub-fields. Image slicing divides the FoV into thin slices and the spatial information is preserved by the system and in the resulting data. Dicing divides the FoV into dices instead of slices and it is usually applied when using microlenses arrays, fiber arrays, microlenses and fiber array combinations and photonic waveguide arrays.

2.3 Pupil Slicing

Slicing is not only performed at image focal planes, it can also be applied to a pupil plane. Slicing the intermediate pupil image provides another way to divide the light from the telescope, meaning the instruments can be smaller and can also be used to divide the wavefront into sub-apertures. The former pupil slicing technique has been employed in the ESPRESSO[5] instrument to increase the spectral resolving power for a given grating parameter set, thereby avoiding the practical limits (e.g. volume, mass, cost, manufacturability, risk) with regards to the gratings, and associated optical components. The latter technique is often employed in wavefront sensing (e.g. a Shack-Hartmann wavefront sensor) for active and adaptive optics (AO) systems.

2.4 "Mode Slicing"

As light passes through the atmosphere its coherence is reduced by refractive perturbations caused by variations in the optical uniformity of the atmosphere. This results in a time variant speckle pattern at the focal plane (interference between the different phases components of the perturbed wavefront) and enlarges the point spread function (PSF) of the telescope. The size of the enlarged PSF is often referred to as the "seeing". In order to couple this light efficiently into waveguide structures, either a large core multi-mode fibers (MMFs) is required, or some kind of mode slicer. A mode slicer (the photonic lantern (PL) was developed for this purpose in astronomy)

Downloaded From: https://www.spiedigitallibrary.org/conference-proceedings-of-spie on 17 Jan 2023
Terms of Use: https://www.spiedigitallibrary.org/terms-of-use

allows an aberrated wavefront to be coupled into a set of single mode fibers (SMFs), by adiabatically converting them from a large multi-mode (MM) group into individual single-modes (SMs). In order to minimize system losses and focal ratio degradation (FRD) in this conversion, the number of modes at the input and the output of the PL should be matched.[6]

As the wavefront coherence increases and the seeing becomes better, smaller fibers can be used, until eventually the diffraction limit is reached and the light can be efficiently coupled into a SMF. SMFs have cores in the range of a few microns, dependent on the optimized wavelength. In order to reach the diffraction limit it is required either a small ground based telescope (where the telescope aperture is matched to the local atmospheric turbulence scales, typically a few centimeters), a highly effective AO system that corrects for the atmospheric perturbation of wavefront, or space based instrumentation that is intrinsically not subject to the wavefront perturbation introduced by the Earth's atmosphere. In such cases, in principle, light can be coupled into a SM waveguide and mode slicing is no longer valuable.

3. TECHNOLOGIES

There are different techniques used in Astronomy to reorganize a 2D FoV and modify its geometrical distribution in order to obtain the spectra of all spatial elements. This can be performed using microlenses, optical fibers, a combination of microlenses and optical fibers, or slicing the FoV with reflective or refractive image slicers. In recent years, photonic technologies have also been used in astronomy (the field of Astrophotonics), such as PLs and reformatters.

3.1 Fibers

Conventional optical fibers allow the "flexible" transmission of light over long distances without the build up of alignment tolerances required with non-waveguide based optical relays such as periscopes. This efficient and flexible relay capability of optical fibers was first used in ground based astronomical instruments to transport light from individual objects in the focal plane to remotely mounted spectrographs in 1978 (e.g. Refs. 7,8). This was quickly followed by the first fiber feed multi-object spectroscopy (MOS), the Medusa plugboard system.[9] Their success and versatile nature led to their rapid adoption in numerous subsequent instruments and they have played a major role in single and multi-object instruments since.

The first prototype of these IFU devices was tested on-sky by Ref. 10. This was then developed into the IFU instrument ARGUS used with the SILFID spectrograph.[11] The ARGUS IFU had 205 active fibers, 169 arranged in a hexagonal pattern to observe the object and an extra 36 fibers set apart from the hexagon in four rows for sky monitoring. All 205 fibers were re-arranged into a slit, to feed SILFID and the system used to observe extended objects. Though it had several flaws lowering the performance (detailed in Ref. 11), it demonstrated the viability of the technology for astronomy applications and several other fiber IFU instruments were subsequently delivered (e.g. DensePak[12,13] and HEXAFLEX[14]). Fiber IFUs systems have also been extended into the infrared (IR), such as the FMOS robotically positioned IR fiber MOS system on the Subaru telescope, which saw first light in 2008.[15] Currently the largest example of this type currently used in astronomy is the VIRUS IFU on HET.[16]

A potential draw back of the conventional fiber IFUs is the relatively low filling fraction as a result of concentric ring structure of optical fibers, with the non-guiding outer fiber cladding ring preventing the fiber cores being located immediately adjacent to each other. Additionally, even a hexagonal close package arrangement of fiber cores has gaps between the cores. Techniques to increase the filling fraction of bare fiber arrays include: stripping the buffer and thereby allowing fibers to be placed closer together and more recently selectively reducing the cladding thickness in the close package hexagonal region to improve the filling fraction as utilized in the SAMI instrument[17] and the upcoming HECTOR[18] instrument.

The major advantage of fiber systems is that they allow the spectrograph to be located far from the telescope focal area. This means they can be placed in a gravity invariant and thermally stable environment, where size and mass issues are typically much less constrained than systems mounted on the main telescope structure. Also with the fiber based systems, the optical fibers intrinsically azimuthally scramble the spatial distribution of the input beam and thereby potentially improving the radial velocity precision of the spectroscopic system,[19] partially mitigating seeing variations, tracking errors and other phenomena that impact the stability of target

Downloaded From: https://www.spiedigitallibrary.org/conference-proceedings-of-spie on 17 Jan 2023
Terms of Use: https://www.spiedigitallibrary.org/terms-of-use

image at the telescope focal plane. Thereby virtually all ground based precision radial velocity spectroscopic systems are fiber fed.

As mentioned previously, the main disadvantages of fiber based IFU systems is that they have a lower filling fraction when compared to other slicing methods. Normal fiber systems have a filling fraction of around 60-65% and hexabundles slightly higher (e.g. in the SAMI instrument the hexabundle IFUs have a filling fraction of 73%). The incomplete filling fraction can make it difficult to sufficiently sample the target being observed. Also fiber systems have a lower throughput at ultraviolet (UV) wavelengths and at wavelengths beyond 2 μm in comparison with other image slicing methods, such as mirrors based IFU. In the thermal IR (i.e. $>$ 1.8 μm) the impact of on the signal to noise of the system can be doubly impacted as low throughput means higher emissivity and potentially a higher thermal background, so not only leading to the lose of signal (lower throughput), but also an increase in noise (increased thermal background), unless the systems are sufficiently cooled (extra cost and complexity). The limitation of the transmission characteristics of suitable materials in the IR region means that virtually all IR images slicing systems are mirror based. Furthermore, standard optical fibers do not maintain polarization. Special SM polarization preserving fibers are available, however, these only transmit a single linear polarization state and being SM require a diffraction limited input for efficient coupling. Therefore, fiber based instruments measuring polarization have to split the light into two orthogonal polarization channels prior to injection into fibers and each output fiber channel must be analyzed separately by the spectrograph (e.g. PEPSI[20]).

3.2 Microlenses

An alternative to an optical fiber array to sample the telescope image focal plane is to use an array of microlenses. This idea was first proposed in 1982[21] and realized by the TIGER instrument.[22] Further developments in the field have been driven by the desire to improve the spatial sampling to resolve the fine details of extended sources. Modern IFUs take advantage of AO that supply a significantly improved quality of the image. This allows the spatial sampling of the instrument to be finer, allowing for enhanced sampling of the field (e.g. OSIRIS at Keck[23]). This is particularly true, with current state of the art instruments including the IFU for SPHERE,[24] GPI IFU[25] and CHARIS (SCExAO).[26] All of these instruments are situated behind extreme AO systems that produce better image correction and therefore finer spatial resolution than standard AO systems. However, it should be noted that such extreme AO systems do not perform optimally in the bluer wavelengths, over a large FoV, or significantly off-axis from the targets (either stars or lasers) used for wavefront sensing.

In a microlens IFU system the native telescope (or AO corrected) FoV is usually optically optimized to match the microlenses via a field expander or reducer lens unit, the microlenses then spatially sample the image focal plane of the telescope with each microlens generating a pupil image at its focal length, associated to the different field point sampled by that lens. The array of pupil images then form the entrance aperture of the spectrograph, where the entrance slit is normally located in a conventional long slit spectrograph. Microlens arrays have also been commonly used as part of wavefront sensing systems (Shack-Hartmann wavefront sensors), were the array of lenses are used to dissect the telescope pupil image (as opposed the scheme above), with each part of the pupil then projected onto a detector array. The location of the image produced by the microlens is then used to determine the tilt of the wavefront at the corresponding telescope sub-aperture.

Microlens array can now be produced by etching, machining or disposing lenses onto a transmissive substrate, including: glass, crystal materials such as sapphire, various polymers and plastics, photoresist, resins or exposes and metals. Most manufacturing techniques produce lenses with same focal length and diameter within a given array, however, custom arrays are possible. Microlens arrays are available with a huge variety of different parameters such as: lenses profile (including: circular, square, hexagonal), lens shape (including: spheric, aspheric, anamorphic, biconic, toric and freeform shaped refractive lenses, as well as diffractive lenses), lens design (including: achromatic and hybrid diffractive/refractive/custom), array formats (including loose packed square, close packed square, loose package hexagonal, close packed hexagonal), lens sizes from a few μm to several mm across, also a large range of focal lengths.

Microlens IFUs generally have a better geometrical coverage, show better transmission, and have better performance in the UV compared with optical fibers,[22] although their performance is not as good as those obtained for optimized mirror based slicer systems. Also, as microlenses are conventional optics, the spectrograph

Downloaded From: https://www.spiedigitallibrary.org/conference-proceedings-of-spie on 17 Jan 2023
Terms of Use: https://www.spiedigitallibrary.org/terms-of-use

fed by the microlens array cannot be located remotely from the telescope focal plane. That imposes design and stability constraints on the spectrograph. In addition, the natural geometry and location of the images produced by the array is limiting, so designers must be careful in order to avoid spectra contaminating each other. This contamination can be due to several reasons, either if there is any cross talk, or due to image/pupil ghosts and other optical aberrations in the system. In addition, microlens arrays do not intrinsically spatial scramble the image information, limiting their application for those science cases requiring high precision/stability spectroscopy, where the removal of spatial information within the spaxel is required.

3.3 Microlenses & Fibers

Some of the disadvantages of solely using fibers or microlenses for an IFU are solved when the two technologies are combined. Inserting microlenses in front of a fiber array can significantly increase the filling fraction of the system as well as optimize the optical parameters (such as focal ratio and image scale) injected into the fibers, i.e. allowing additional control of the system etendue. The microlenses can either inject a pupil or focal image into the fibers. There are potential pros and cons with either technique, however, we do not explore these in this paper. Microlenses can also be used at the optical fiber output, i.e. the entrance of the spectrograph, to accommodate the focal-ratio and place the exit pupil at the desired position for the spectrograph.

One of the early facility class IFUs to use the combination of microlenses and fibers was the Gemini Multi-Object Spectrograph (GMOS)-IFU[27] that was designed to provide an IFU mode for each of the Gemini South and Gemini North GMOS instruments. This was an extremely compact IFU, necessitated by the need to fit into the multi-aperture (slit) wheel of the GMOS instrument, in which the input and output of the IFU needed to be in the same plane (i.e. the GMOS slit mask focal plane). The GMOS IFU had a 2D array microlenses that sampled the input telescope image and coupled light into a looped fiber bundle that reformatted the field into linear array of fibers at output. This then fed linear microlens arrays that formed a pseudo-slit acting as the entrance aperture of the GMOS spectrograph, as well as optimizing the light coupling and alignment at the spectrograph pupil. Concurrently, the SPIRAL and prototype SOAR microlenses/fiber based IFUs where being developed for the Anglo-Australian telescope (AAT) and SOAR telescope respectively. During the late 1990s, a near infrared (NIR) optimized microlens and fiber based IFU, called the SMIRFS-IFU,[28] was developed to feed the United Kingdom infraRed telescope (UKIRT) J, H & K band CGS4 spectrograph. More recently several other instruments have incorporated microlenses and fiber based IFUs, such as VIMOS,[29] PMAS[30] and IMACS-IFU.[31]

The combination of microlenses and fibers typically have a lower throughput than simple microlenses, but provide the versatility in field reformatting, scrambling and remote spectrograph mounting. They also allow the higher input filling fraction provided by microlenses arrays, as well as the etendue management/manipulation that enables optimized light coupling between input and output and propagation within the fiber. However, like the simple microlens array based IFUs such systems can be limited by microlens manufacturing technologies and intrinsic optical quality of the microlenses. In additional to transmission losses in the microlens array and optical fiber, there can be additional losses due to FRD in the fibers[32] and significant scattered light issues have been noted with microlenses,[33] leading to coupling loss and contributing to crosstalk between adjacent fibers. All these effects reduce the signal to noise sensitivity possible with such systems.

3.4 Image Slicers

The first image slicer was developed by Bowen in 1938[34] as a device to reduce the light loss at the slit of a spectrograph by reformatting a circular image into a linear shape (entrance slit) providing more efficient coupling into the spectrograph. The first references with regards the use of image slicers in astronomy were based on modified versions of the Bowen-Walraven slicer[35].[36] These, together with the MPE imaging spectrometer,[37] were the concepts developed in the XXth century. In the XXIst century, several advances were deployed in the field, in systems such as: SPIFFI[38] in the VLT SINFONI instrument, the Florida Image Slicer for Infrared Cosmology and Astrophysics (FISICA),[39] MIRADAS[40] for GTC telescope or the image slicers of KMOS[41] and MUSE,[42] the Multi Unit Spectroscopic Explorer. Most recently, innovative image slicer designs have been employed that control the symmetry to overlap all intermediate pupil images;[4] combine the elements of the IFU with those of the spectrograph[43] or offer a collimated output beam.[44]

Downloaded From: https://www.spiedigitallibrary.org/conference-proceedings-of-spie on 17 Jan 2023
Terms of Use: https://www.spiedigitallibrary.org/terms-of-use

The typical image slicer based IFU uses an array of mirrors (slicer mirror array) with different orientations located at the image focal plane.[4] This mirror array reflects each slice of the image in a different direction. Other mirror arrays are used to control the angles, produce an intermediate pupil image, focus the images of the slices of the FoV generating one or more pseudo-slits and control the position of the exit pupil for the optimum coupling between IFU and spectrograph.

In an image slicer, the number of arrays depends on the design; the number of mirrors per array is related to the FoV and the width of the slicer mirrors defines the sampling. Also, since it is directly related to the slit width, it contributs to the spectrograph spatial and spectral resolutions.

The efficiency of an optimized image slicer depends on the mirror surfaces (i.e. their reflectivity, surface roughness, surface figure). The reflectivity of the coating is optimized to match the required spectral range. Thus, for IR systems, a coating of Gold, Protected Gold or Protected Silver are typical chosen, while for visible wavelengths Aluminum or Silver are typically preferred. The reflectance of such metallic coatings can be further improved adding a dielectric overcoat (protected coatings) or several dielectric layers combining high and low refractive index (enhanced coatings). Image slicers can be manufactured in glass or metal, as monolithic pieces or individual mirrors assembled. Currently, the thinnest manufactured slicer mirrors have a width of 100 μm in glass, these were developed by Winlight Optics[4] and 33 μm in metal, developed by Canon.[45]

Some of the advantages of using mirror based image slicers are: the system etendue is conserved and it can be controlled to facilitate the optimum coupling with the spectrograph, as well as to define the effective size of the output slit or slits; the orientation of the mirrors is fixed and therefore polarization information is conserved/stable, unlike fiber based systems (unless the polarization states are split into two separate fiber channels). However, since the orientation of the mirrors is fixed, this limits the shape and size of the FoV and, therefore, image slicers are not typically suitable to be used as a MOS IFU system, unless an upstream system is used to reorganize the images of the observed objects in a FoV with the same dimensions and shape of the FoV for which the image slicer was designed, such as pick-off relay/s. Such pick-off have been used in the KMOS instrument,[46] but it has a complex optical system with over 300 separate optical paths.

3.5 Photonic Lanterns and Reformatters

The photonic lantern was first developed in 2005 to enable SM to MM conversion.[47] It was created by filling a photonic crystal fiber (PCF) with SMFs. This combination was then heated and drawn down into a tapered section in which to SMF become progressively smaller and light can start to couple between adjacent SMF cores. Eventually towards the smallest end of the taper the SMF cores became so small that they no longer efficiently guide light and the region effectively behaves like a standard MMF. Since then multiple configuration and manufacturing methods have been developed for producing PLs with optical fibers[6] and bulk waveguide. The latter is a new method developed to create the devices by directly writing waveguides into a glass block,[48] using ultrafast laser inscription (ULI) to make a positive refractive within the substrate. The refractive index structures that have been written into the glass then act as waveguides within the glass block, in the same fashion as the fiber cores in the fiber based PLs.

The development and basic architecture of the PL also opened up possibilities to reformat the shape of the PL output by re-arranging the individual single modes cores, into a linear array for example. Such devices, have become known as photonic reformatters and function in a similar way to an image slicer by re-arranging an input into a linear output array. Various groups have now manufactured devices using first ULI inscription in glass slabs and more recently by re-arranging the positions of the fibers[49] or a combination of fibers and ULI inscribed waveguides.[50] So far all examples of PLs and photonic reformatters use in astronomy have been development prototypes, with examples such as the Photonic TIGER[51] and GNOSIS[52] and the photonic dicer.[53] The next generation of photonic instrumentation is currently being built, with instruments such as PRAXIS being commissioned in the near future.[54]

The primary advantages of the PL and photonic reformatters are: they can be fully integrated devices, can be relatively simple to manufacture and align (compared to alternative technologies), the fabrication techniques can be combined to take best advantage of each technology, they can also be combined with existing technologies, and because the PL converts the input from MM into SM then numerous photonic techniques/methods for

Downloaded From: https://www.spiedigitallibrary.org/conference-proceedings-of-spie on 17 Jan 2023
Terms of Use: https://www.spiedigitallibrary.org/terms-of-use

light manipulation become viable/accessible. A good example is the inclusion of fiber bragg gratings (FBGs) into the devices to suppress the night sky background.[55] Indeed, it was for this latter purpose that the PL was initially developed. However: the development of PLs and reformatters are still in the early stages, with all being prototype (as opposed to facility class) instruments; the technologies have similar wavelength limitation to conventional fibers (for PLs and reformatters this is currently limiting these development to optical and NIR application, though some research is being performed to develop devices in the mid infrared (MIR)); the loss per unit length of ULI glass block devices is still high in comparison to optical fibers and conventional optics.

4. DISCUSSION FOR DIFFERENT ASTRONOMICAL CASES

The suitability of a reformatter alternative to given applications depends not only on its capabilities, but also on the expected image quality/conditions and characteristics of the intended target or source. Three ground based telescope image quality scenarios are explored in this section:

- Natural seeing conditions
- Partial AO corrections
- Diffraction limited conditions

Each of the conditions have also been addressed for studying point sources (where retention of spatial information is redundant) and extended sources (where the preservation of spatial information may be required).

The general functionality/advantages/disadvantages of mirror based, fiber based and PL based reformatting systems are summarized below. The detailed trade-offs are outlined in each of the scenario sub-sections.

As described in Section 3, mirror based image slicers can provide reformatting with anamorphic or regular magnification and the conservation of etendue. They can preserve polarization information and the mirror coating can be optimized to maximize the throughput over the desired spectral range. Their application can improve the spatial and spectral resolving power, but in a fixed pixel system this comes at the cost of reducing the available multiplex or FoV possible with any given system.

Optical fibers offer flexible and remote reformatting with multiple input and output geometrical distributions possible. Like mirror based slicers, they can be deployed to increase the spatial and spectral resolution of any given system configuration. They provide a degree of spatial scrambling, potentially increasing the accuracy and stability of precision spectroscopy applications. Fibers can also act as spatial filters by removing higher order wavefront terms from the propagating light, if the modes preferentially excited by those terms are not efficiently propagated by the fiber. The extreme of this phenomena is the SMF, which only supports the fundamental mode (i.e. the component of the coupled light that is diffraction limited). However, MMFs can degrade the system etendue, via a mechanism called focal-ratio degradation (FRD), and standard fibers do not intrinsically conserve polarization information. Bare fiber arrays are somewhat limited in terms of maximum filling fraction and can have a limited transmission efficiency toward the UV and MIR spectral ranges.

Fiber based PL reformatters are very similar in performance to optical fibers, but with the following differences: It is possible to embed photonic functions such as narrow band filtering with FBGs; improve the spatial and phase scrambling; from a MM input, the PL output can be reformatted into a narrow spectrograph entrance slit. At the extreme limit this slit width can be reduced to such an extent that it becomes diffraction limited. Glass block based PL reformatters offer the same functionality as fiber based PL reformatters, though they are typically much more compact, but show higher losses and are not able to reformat or to couple directly to remote instrumentation. Hybrid PLs that combine fiber and glass block components can utilize the advantages of both technologies. It should be noted, however, the complexity of PL reformatters scales directly with the number of modes required to efficiently couple the input beam. Also, there is not a simple correspondence between the input wavefront and the distribution of light within the cores of the PL. That said, there has been some limited success in deconvolving the wavefront information from the mode energy distribution in the few mode cases.[56]

Microlenses arrays could be used to couple light into or out-of both standard optical fiber and fiber based PL reformatters, either pupil or image coupling light into the device as previously outlined.

Downloaded From: https://www.spiedigitallibrary.org/conference-proceedings-of-spie on 17 Jan 2023
Terms of Use: https://www.spiedigitallibrary.org/terms-of-use

4.1 Natural seeing conditions

Natural seeing describes the conditions at a typical ground based telescope (i.e. the primary mirror aperture is significantly larger than the atmospheric coherence length) without AO correction, where the image quality is typically dominated by blurring produced by the atmospheric turbulence and the achievable spatial resolution is greatly reduced. The seeing also impacts the pupil, where it introduces high level aberrations.

The parameters of significance for the different reformatting technologies are:

- Image size (field reformatting)
- Wavefront shape (pupil formatting)
- Number of waveguide modes for optimal performance.

4.1.1 Point sources

The main function that is required of a reformatter in these conditions would be field and/or pupil slicing in order to reduce the effective slit width and thereby increase the spectral resolving power of a given spectrograph design, or splitting of the polarization into orthogonal states for spectrograph-polarimetric applications. Any of the reformatting technologies could be used, however, for large telescope apertures and bluer wavelength regimes, the number of mode in the PL based device will become challenging and eventually impractical (see Fig. 4).

4.1.2 Extended sources

The function required from a reformatter in these condition is similar to those for point source case above, but likely with the added requirement of preserving spatial information and enabling the processing of each region (spaxel) separately. That means, therefore, that more information being simultaneously collected and processed, so the issue of managing the number of modes become even more challenging for PL based devices.

4.2 Partial AO correction

Partial AO correction describes the condition in which the seeing limited telescope performance is corrected to some extent, but not sufficiently to achieve the ultimate diffraction limit. It can provide significantly better image quality (or pupil wavefront uniformity) than natural seeing, but does not achieve the best possible image quality (or uniform pupil wavefront) for space based application (i.e. without any atmospheric perturbation). The AO system redistributes the light within the PSF, usually with the goal of either concentrating as much light as possible into the central region of the image, or to maximize encircled energy within a given aperture. However, due to limitation in the wavefront correction, particularly these very high order, rapidly changing components, the systems cannot typically fully correct the light distribution in the wings of the PSF. The resulting PSF can then have a well defined/corrected central region, but significant energy in the extended wings, which can contribute considerable background/noise at the focal plane. In term of the pupil wavefront the AO system can correct much of the lower order wavefront aberrations, but not the very high order perturbations.

4.2.1 Point source

For the observation of a point source under the conditions of partial AO correction, the characteristics associated to reformatting with mirrors, optical fibers and PLs are similar to that in natural seeing conditions. However, the image size (or pupil wavefront aberration) should be reduced, possible by a huge amount, reducing the size, complexity and number of modes required to effective sample the image (pupil wavefront). Furthermore, the additional spatial filtering function possible with optical fibers and PLs can be utilized to remove/clean the wings of the PSF (residual high order wavefront errors) and improve the single to noise capacity of the system. Unfortunately the spatial and phase scrambling functionality of fibers and PLs is inversely proportion to the number of modes support in the system so as the AO correction improves the spatial scrambling and modal noise of the system typically degrades. However, it should be noted that the mirror based units do not provide any spatial or phase scrambling functionality.

Downloaded From: https://www.spiedigitallibrary.org/conference-proceedings-of-spie on 17 Jan 2023
Terms of Use: https://www.spiedigitallibrary.org/terms-of-use

4.2.2 Extended source

The function required from a reformatter in these condition is similar to those for point source case above, but typically with the added requirement of preserving spatial information. The issue of managing the number of modes in PL based devices can be much less that for the seeing limited case as the number of mode supported can have been drastically reduced (see Fig. 4).

4.3 Diffraction limited conditions

Diffraction limited conditions can occur if: (1) the telescope is space based. This can be achieved if the telescope aperture is close to or smaller than the local coherence scale of the atmosphere (as the coherence scales with wavelength, as you move to longer wavelengths it is easier to achieve the diffraction limit); (2) there is a highly effective AO system (such systems are often referred to as Extreme AO system on large telescopes).

4.3.1 Point source

The observation of point sources in diffraction limited conditions does not require reformatters and there is no advantage in slicing or dicing the field (or correcting an already uniform wavefront). PLs are redundant as you can efficiently couple light into a SMF and impose photonic functions such as FBG based filtering without degrading the device's performance.

4.3.2 Extended source

Diffraction limited extended sources have the same requirements as diffraction limited point sources, however, preservation of spatial information is a likely requirement and reformatting may be desired. Either mirror based or single mode fiber based devices could be used, but PL based devices would inappropriate as the MM to SM functionality is redundant in the diffraction limited case.

5. PHOTONIC SLICERS

As discussed in Section 3, there are many different reformatting alternatives, each having some advantages and disadvantages. The goal of this research is to investigate the feasibility of an hybrid reformatter/IFU combining conventional optics with photonics in order to benefit from the advantages of both.

As highlighted in the previous section, the size of the telescope aperture and the resulting level of wavefront aberration have a profound impact on the size and complexity of photonic solutions. For the concept described in this section, it has been assumed that the mode number is high (i.e. large aperture telescope, partial or no AO correction), so solutions that have photonic reformatting within the PL structure have not been considered as the slit length would become impractical. However, for applications with lower mode numbers, such configuration would be feasible.

Our proposal is called the photonic slicer (PS) (Fig. 2) and it is composed of an image slicer (dicer) placed at an image focal plane; an array of PLs for MM to SM conversion and a second array of PLs to combine the light back into MM fibers and generate the spectrograph slit. Thus, as presented in Fig. 3, we pass from MM single-core at the entrance of the first PL, to SM multi-core in an intermediate plane, to MM single core again. And the reason why we produce this double transition is to include photonic functionalities not available when using conventional image slicers, such as: reduction of the influence of OH lines; spatial scrambling or spectral and spatial filtering.

In this hybrid IFU proposal, an image slicer dices the PSF at the telescope image focal plane and generates an image of each dice with the size defined by the core of the PLs in the input PL array. The required magnification to match the telescope that is optimal for the PL array is produced by the mirrors of the image slicer. The output of the image slicer does not need to be a slit, as in conventional optics, in this case the output distribution is defined by the distribution of the input array of PLs.

Diffraction limited optical quality is not required, however, a uniform optical quality across the field would reduce the number of modes required to propagate in each PL and thereby simplifying the system. Since a good optical quality is not required, this proposal counts on more flexibility in the output angles of the image slicer

Downloaded From: https://www.spiedigitallibrary.org/conference-proceedings-of-spie on 17 Jan 2023
Terms of Use: https://www.spiedigitallibrary.org/terms-of-use

with respect to pure image slicers IFUs, allowing several possibilities that can fit in the available volume and for specific geometrical distributions. Some examples are presented in Figs. 5 and 6.

Photonic lanterns can be used for observations whose conditions are far from the diffraction limit. The cases contemplated, as discussed in Section 4, are: natural seeing or partial AO corrections, as no benefit has been identified for such a design in the diffraction limited regime.

The output of the image slicer is then coupled to the input array of PLs, using a single PL per dice. The input array of PLs performs the transition from MM to SM, minimizes modal noise and introduces photonic functionalities. In the photonic slicer proposal, these PLs are used to spatially filter the PSF from the image slicer and scramble the near and far field image to reduce the impact of input coupling instability/variations that can propagate through the system that do not effectively scramble the image structure. The second array of PLs produces the inverted conversion, from SM to MM.

Although a PL is not a reformatter, an array of PLs can function as a reformatter by organizing the PL outputs into a linear array, thereby forming the spectrograph entrance slit. The width of the spectrograph slit is defined by the core size of the MM section of the PLs that form the slit. The core size of the output PLs do not need to be the same as those of the input PL array, as long as the etendue is conserved (ensuring minimal system losses). Thus, a combination of PLs for both input and output arrays can be selected to define the magnification from the image slicer output to the spectrograph input. The length of the spectrograph slit is related to the core size and separation of the output array of PLs and the number of dices (set by the FoV and spaxel size requirements), which defines the number of PLs required.

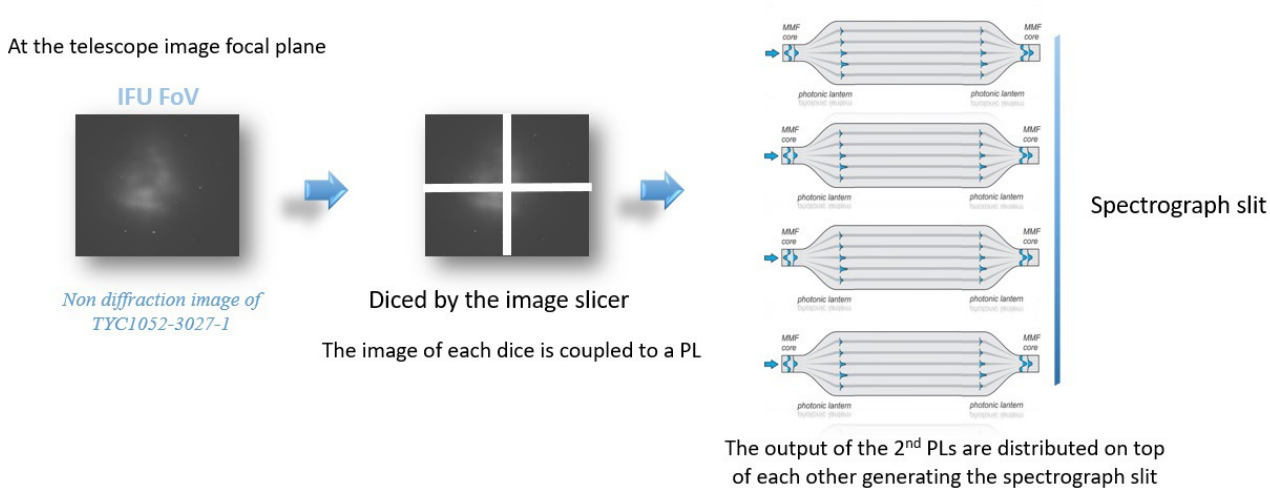

Figure 2. Sketch of the photonic slicer (PS) composed of an image slicer and two arrays of photonic lantern (PL). An image slicer dices a non diffraction limited image at the telescope focal plane and generates an image of each dice with the size required by the core of the input array of PLs. The first array of PLs produces the multi-mode (MM) to single-mode (SM) conversion, avoiding modal noise and allowing the introduction of photonic functionalities. The output array of PLs is used to return to MM and generate the spectrograph slit by arranging the PLs into a linear array.Only four dices have been represented to explain the concept.

Image slicers can be designed to be extremely efficient over a broad wavelength band and optimize the image quality, which is essential to minimize the number of modes within the PL. The size of the slicer/dicer mirrors would be larger than the typical ones used for high resolution IFS, thus, this does not imply any technological complexity and, since the proposed design is developed for the IR spectral range, the slicers can be made in metal, reducing the costs. In this hybrid solution, the size of the dicer mirrors define the spaxel, without needing any additional anamorphic system.

Downloaded From: https://www.spiedigitallibrary.org/conference-proceedings-of-spie on 17 Jan 2023
Terms of Use: https://www.spiedigitallibrary.org/terms-of-use

A mirror based image slicer was considered instead of microlenses since these are chromatic and, although the current proposed spectral range is not too large, from 1 to 1.8 μm, the idea is to extend it as much as possible, which leads to an achromatic solution. Image slicers can be designed to offer a uniform optical quality across the defined FoV, however, in order to do this with microlenses, the characteristics of the lenses on-axis and on the borders of the array should be different, increasing the complexity of the lenslet array manufacturing. Reflective image slicers offer more flexibility in the magnification with a better control of the aberrations by the application of off-axis aspheres or freeform optics. Another advantage of using image slicers is the flexible output, which can be adapted to different geometrical distributions facilitating the coupling with the PL in those cases in which the geometry of the available volume is restricted.

The efficiency of the PS is the product of the efficiency of the image slicer and that of the input and output arrays of PLs. The efficiency of an image slicer depends on the number of optical surfaces, the coating and the wavelength. For this throughput estimation, a conservative efficiency of 92% was considered, however, the efficiency of an image slicer can be higher than this. The efficiency of a PL is primarily driven by material losses and any mismatch of the mode count either side of the transition regions. In the optimal case it can be around 90% at the design wavelength. This leads to a total efficiency of about 75% for the photonic slicer, which includes a number of advantages with respect to conventional image slicers, summarized below:

- Stability of the output PSF, for high precision Spectroscopy.
- This IFU proposal is suitable for remote mounted spectrographs, which offers: stability, gravity invariance and also environment invariance, since the spectrograph could be in a temperature controlled room.
- Embedded functionality: spectral filtering for OH lines reduction and unwanted emission contribution from the IR night sky.
- Spatial filtering that allows to obtain a clean PSF, reducing the noise and improving the signal-to-noise.
- And the spaxel would be defined by the dicer mirrors, without needing any additional anamorphic relay.

5.1 Potential application for the Extremely Large Telescope

A specific potential use case or application of the PS for the Extremely Large Telescope (ELT)[57] was studied, this was focused on the instrument HIRES.[58] Some preliminary analyses were performed to consider sizes, focal lengths and possible critical points found during this initial study.

In the modal picture the optimal coupling is set by matching the number of fiber modes for the required wavelengths. For a given telescope (in native seeing condition as expected with HIRES) this is related to the FoV covered by the slicer and the wavelength. PLs are usually manufactured using a series of hexagonally symmetric rings (having 1,7, 19 cores etc), though theoretical work has shown that optimal modal evolution is not necessarily achieved in this fashion.[59] For our study we have access to several MCFs, these have 73, 121 and 511 cores. In order to select the optimal fiber core number we use Fig. 4, which shows the number of modes for given FoV per slice, this means the FoV covered by each slicer mirror, and wavelength. The 511 core fiber was selected for two reasons, firstly it is designed perform efficiently over a broad wavelength range (approximately an octave)[60] and secondly as the PSF produced by the Extremely Large Telescope (ELT) will be close to seeing limited.

Assuming a central wavelength of 1500 nm, that means the FoV needed per slicer mirror is approximately 0.22 arcseconds over our selected wavelength range of an octave. In order to match the fiber size to the telescope a numerical aperture (NA) of 0.23 was considered, which corresponds to a focal-ratio of F/2.17. Normal fiber systems are normally fed with a slower beam as standard MM optical fibers have a NA of 0.22 or less. However, with PL devices we are able to tune the input/output NA by the choice of cladding material for the transition/MM section of the PL. For our concept, the faster beam produces a smaller image on the fiber, meaning alignment

Downloaded From: https://www.spiedigitallibrary.org/conference-proceedings-of-spie on 17 Jan 2023
Terms of Use: https://www.spiedigitallibrary.org/terms-of-use

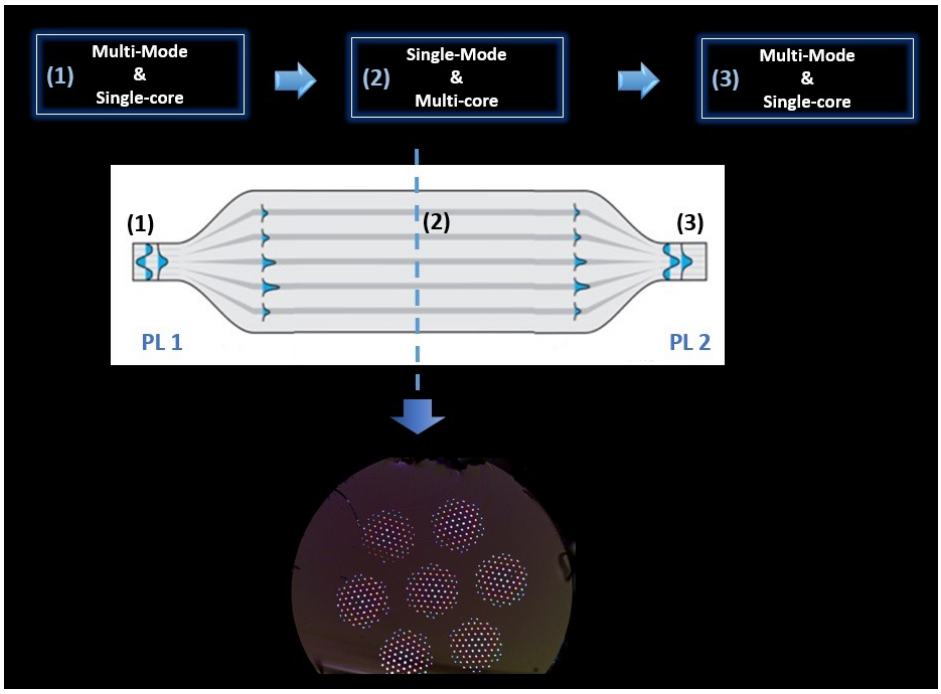

Figure 3. The coupling between the two arrays of PL allows a double modal transisition. The first array of PL allows the transition from MM single-core to SM multi-core, allowing to include photonic functionalities, such as: reduction of the influence of OH lines; spatial scrambling or spectral and spatial filtering. The second array of PL produces the inverted transition, from SM multi-core to MM single-core. The fiber shown here is an example of an 511 core multi-core fiber (MCF) designed for visible light. For our study the cores would be a larger size in order to guide the light better.

tolerances would be tighter, but reduces the susceptibility of the transition region to losses as a result of external perturbations.

As the MM section of the PL acts like a standard step index MMF , we can use Equation 1 to calculate the number of modes.

$$M = \left(\frac{V}{2}\right)^2 = \left(\frac{\pi d NA}{2\lambda}\right)^2 \tag{1}$$

Here V is thought of as a normalized optical frequency, d the diameter of the fiber core, NA is the numerical aperture of the fiber and λ the wavelength. Taking our NA and a central wavelength of 1500 nm, then re-arranging equation 1 and calculating for d yields a core diameter of 94 µm.

In order to achieve a sampling of 0.22 arcseconds/slice (0.22 x 0.22 arcseconds per dice) and taking into account that the telescope plate scale is 3.31 mm/arcseconds, the FoV must be divided in dices of 0.73 mm x 0.73 mm. The input focal-ratio for the image slicer is the telescope output focal-ratio, which, for the ELT, is F/17.7. The output focal-ratio of the image slicer is defined by the NA of the input array of PLs, F/2.17 in this case, implying a magnification of 0.12.

The size of the images produced by the image slicer at its image focal plane is 0.087 mm, 93% of the size of the core leaving some margins to avoid light losses in case of misalignments. The specification considered for the preliminary design study are shown in Table 1.

The first image slicer layout considered was a MUSE-like design since it uses the minimum number of optical surfaces. Only two powered mirrors would be required in this case, a powered slicer mirror and a powered camera mirror per slice to focus the beams generating the PL's entrance. The second optical surface, the camera mirror, produces the required magnification and controls the image position defined by the PL location. The use of

Downloaded From: https://www.spiedigitallibrary.org/conference-proceedings-of-spie on 17 Jan 2023
Terms of Use: https://www.spiedigitallibrary.org/terms-of-use

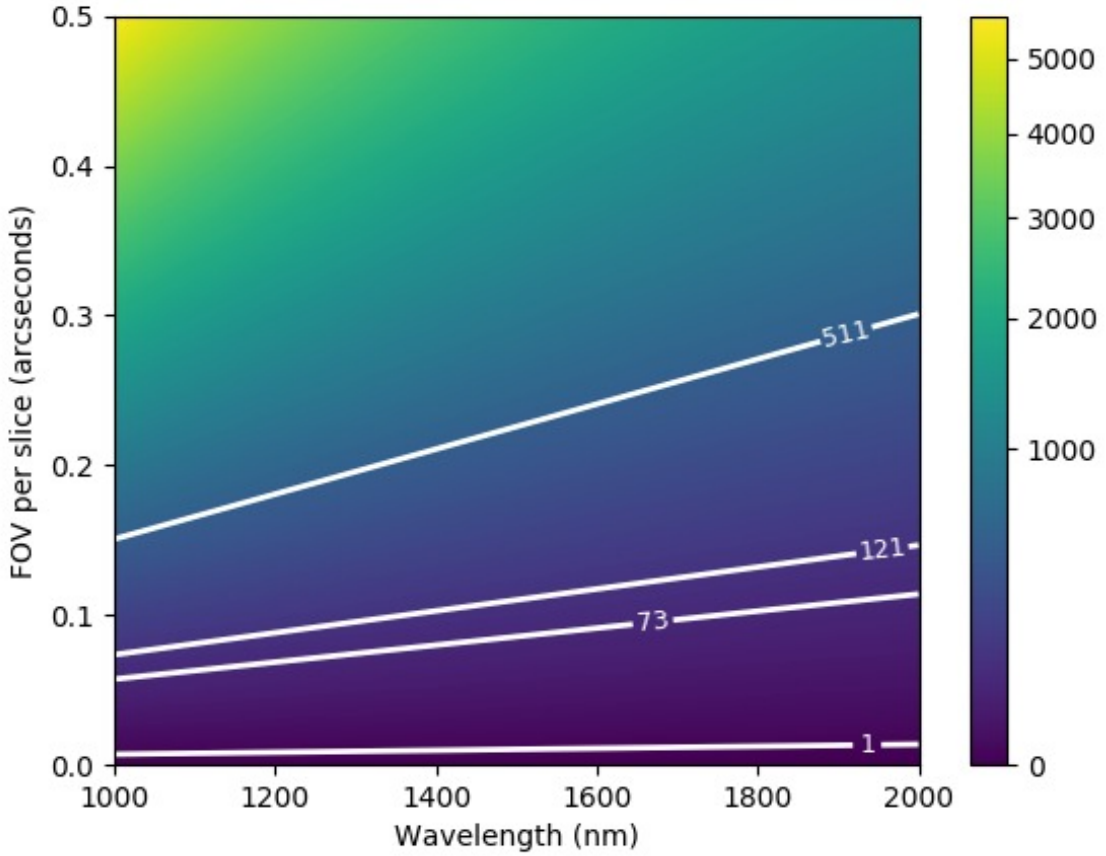

Figure 4. A graph showing the dependence of the number of modes (not including polarization) on both field of view per slice and wavelength. The contours correspond to our available fibers (including a single mode fiber suitable for use at the diffraction limited) and show the optimal wavelength and field of view for that fiber. The color bar is scaled as the square root of the number of modes.

Table 1. Specifications considered for the preliminary design study.

Sampling	0.22 arcseconds/dice
Slicer mirror width	0.73 mm
Input F/D	F/17.7
Output F/D	F/2.17
Magnification	0.12
Slicer image size	0.087 mm

an even number of mirrors ensures light propagation away from the telescope in the original direction of the telescope output beam.

The preliminary layout was designed in Zemax using the the ELT Zemax optical design model as the input. The image size at the ELT image focal plane is 6.8 mm x 6.8 mm, which can be fully covered with 10 x 10 dicers. Only 4 dicers were initially modeled for this preliminary feasibility study. Five field points per dicer were defined

Downloaded From: https://www.spiedigitallibrary.org/conference-proceedings-of-spie on 17 Jan 2023
Terms of Use: https://www.spiedigitallibrary.org/terms-of-use

covering the center and extremes of each dice. The different combinations of focal lengths for the two image slicer components provide the required magnification of 0.12. For the first study a focal length of 500 mm for the slicer mirrors and 60 mm for the camera mirrors was considered. Both mirrors were chosen to be spherical for this first analysis, although off-axis aspheres or freeform optics could offer better optical performance should it be desired.

The output parameters of the image slicer are flexible and the position of the generated images can be adapted to match the PL. The geometry of the design is also flexible and the output could be arranged in several different ways. Two design alternatives are shown in Figs. 5 and 6. Four slicer mirrors are dicing the image at the telescope focal plane. Each mirror has a different orientation (Tilt about X and Tilt about Y axes) to drive the beams towards the camera mirrors. In Fig. 5 the camera mirrors generate images in between the two rows of camera mirrors leading to a PL position integrated in the volume covered by the image slicer, ensuring a compact systems footprint. The image slicer can be designed to generate the output images well away from its own optical path to avoid possible vignetting. An example is shown in Fig. 6 where the images of the dices are generated on a side of the image slicer layout.

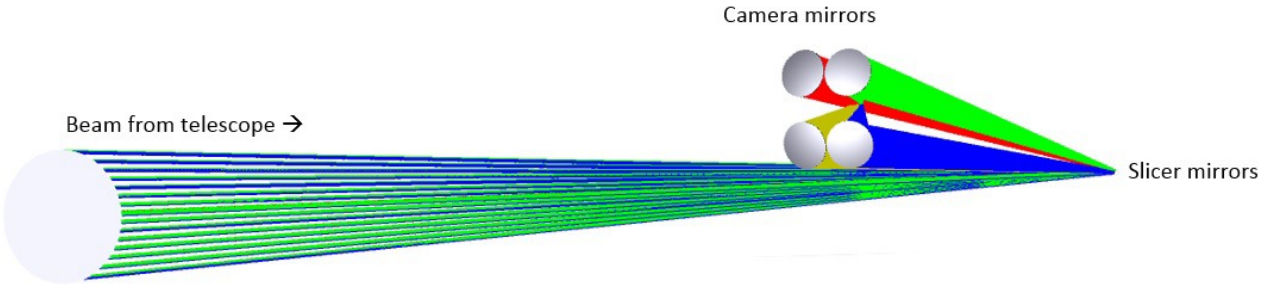

Figure 5. Design alternative with only four dices of the field of view arranging the image slicer output to be placed between the camera mirrors. The slicer and camera mirrors are spherical with 500 mm and 60 mm focal length, respectively. The camera mirrors produce a magnification of 0.12.

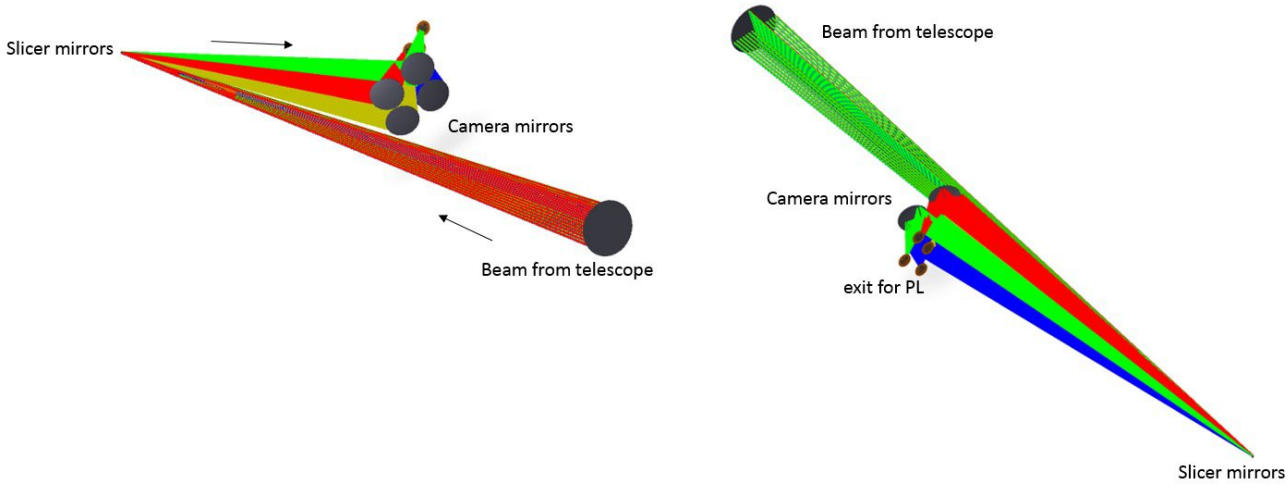

Figure 6. Design alternative of an image dicer where the output images, exit for photonic lantern coupling, are displaced laterally avoiding potential vignetting with the image slicer beams. The camera mirrors produce a magnification of 0.12.

The PL does not require diffraction limited image quality at its input, however, homogeneous optical quality across the field would reduce the number of modes necessary in any given PL and thereby simplify the system.

Downloaded From: https://www.spiedigitallibrary.org/conference-proceedings-of-spie on 17 Jan 2023
Terms of Use: https://www.spiedigitallibrary.org/terms-of-use

The layouts of Figs. 5 and 6 were developed as a feasibility study and to evaluate the potential limitations to the dicing optics that have to be taken into account in future designs. Considering the angles and off-axis distances, spherical mirrors are not the best choice due to inherent aberrations. In a design like this, focal lengths should be short enough to reduce the camera diameters and consequently, minimize the tilt angles, but also large enough to take the exit beams away from the image slicer optical path for the PL coupling. The magnification was generated using only the mirrors of the image slicer in order to optimize the throughput, however, the magnification of 0.12 that transforms an F/17.7 beam into an F/2.17 produces aberrations, which in our case are dominated by coma. The optical quality can be improved by considering: the image slicer layout, this means the potential incorporation of more surfaces in the image slicer; focal lengths and sizes that are related to off-axis and tilt angles and different conic surfaces, such as off-axis aspheres or freeform optics. A trade-off analysis between the maximum FoV that can be covered with a uniform optical quality and the maximum demagnification should be done considering the resulting number of modes.

6. CONCLUSIONS

The use of Integral Field Spectroscopy (IFS) in astronomy is extremely powerful. The science cases for the next generation of spectrographs demand larger field of view (FoV) coverage with high stability and high spatial and spectral resolving power. During recent years, the spectroscopic capabilities have been significantly improved by new technological developments. A highly successful and regime changing developments has been field reformatting, enhancing the conventional Spectroscopy (long-slit Spectroscopy) and enabling the new era of information reach Integral Field Spectroscopy (IFS).

In Integral Field Spectroscopy, Integral Field Units (IFUs) are used to reorganize a bi-dimensional FoV into one or more long slits. Although this reorganization is the main functionality of an IFU, the advances developed during the last years have led to systems/technologies that can add additional functionalities: change the shape and size of the FoV; control the sampling; control the spatial and spectral resolving power; enhance scrambling to stabilize the spectrograph line profiles and enhance measurement precision; modal decomposition; spectral and spatial filtering to remove unwanted background; efficiently transport the light from the telescope to remotely located instruments or adapt the optical parameters to match the input and output requirements whilst maintaining the system etendue. Now there are several technologies platforms to reformat the FoV and enable these functions using conventional optics (microlenses, fibers, image slicers), photonics (photonic lanterns (PLs) or photonic reformatters) and/or hybrid combinations. Each architecture will have some advantages and disadvantages for a given application and our proposal is a combination of conventional optics and photonics in an hybrid IFU that combines some advantages of both. The proposal is called the photonic slicer (PS) and is comprised of an image slicer (dicer) at the telescope image focal plane plus two arrays of PLs. The image slicer dices the telescope point spread function (PSF) generating an image of each dice with the size of the core of the array of input PLs. This array of input PLs provides the conversion from multi-mode (MM) to multiple single-mode (SM) components. The array of output PLs converts the multiple SM components into a single core MM output. The double transition enables photonic functionalities, not available in conventional image slicers.

Some of the advantages of the Photonic Slicer are note below:

- Stability of the output PSF, for high precision Spectroscopy.
- As the PL can be fiber based, this IFU alternative is suitable for remote mounted spectrographs, offering: additional stability, gravity invariance and also environment invariance as the spectrograph can be located in a temperature controlled room.
- Embedded functionality: spectral filtering for OH lines, which removes unwanted narrow line emission contributions from the infrared (IR) night sky.
- Spatial filtering that allows to obtain a clean PSF, remove the contribution of the wings and thereby reducing the background contamination sources to improve the signal-to-noise.

Downloaded From: https://www.spiedigitallibrary.org/conference-proceedings-of-spie on 17 Jan 2023
Terms of Use: https://www.spiedigitallibrary.org/terms-of-use

- The spaxel can be defined by the dicer mirrors, without needing any additional anamorphic relay, keeping the design simple and efficient.

A preliminary study for a potential application to the Extremely Large Telescope (ELT) was developed to evaluate possible design limitations. The initial design of the image dicer considered an F/17.7 input beam that was transformed into an F/2.17. The dicer mirrors have a size of 0.73 mm x 0.73 mm equivalent to 0.22 arcseconds x 0.22 arcseconds. The design of the image dicer used two spherical mirrors. Although the PL does not require diffraction limited optical quality, an homogeneous optical quality across the field would reduce the number of modes simplifying the system. In the initial design alternatives the optical performance is dominated by coma, which can be improved using different conic surfaces, such as off-axis aspheres or freeform optics and with control of focal lengths, sizes and magnification.

The PS has a estimated efficiency of about 75%. The spectral range currently considered extends from 1 to 1.8 μm, however, this could be extended into the visible regime and to longer wavelength by considering different fiber materials.

It is currently envisaged that the main potential applications of the PS are high precision spectrographs and Integral Field Spectrographs that require ultra-stability, like ESPRESSO[5] or HIRES[58] or spectrographs whose science cases include the observation of faint sources. However, the proposal is still in an early stage and further investigations will be made within OPTICON in the next two years, including the development of a proof-of-concept prototype.

ACKNOWLEDGMENTS

The authors wish to thank Sam Barden for the information with regards the historic use of optical fiber in astronomy (Private Communication). Robert J. Harris and Roger Haynes are supported by the Deutsche Forschungsgemeinschaft (DFG) through project 326946494, 'Novel Astronomical Instrumentation through photonic Reformatting'. This project has received funding from the European Union's Horizon 2020 research and innovation program under grant agreement No 730890. This material reflects only the authors views and the Commission is not liable for any use that may be made of the information contained therein.

This research made use of Numpy[61] and Matplotlib.[62]

REFERENCES

[1] A. Calcines, M. Collados, A. Feller, *et al.*, "Spectrograph capabilities of the European Solar Telescope," in [*Proc SPIE*], **7735**, 773520 (2010).

[2] A. Calcines, R. L. López, and M. Collados, "A high resolution integral field spectrograph for the european solar telescope," *Journal of Astronomical Instrumentation* **2**(1) (2013).

[3] F. Laurent, E. Renault, H. Anwand, *et al.*, "MUSE field splitter unit: fan-shaped separator for 24 integral field units," in [*Proc SPIE*], **91511U** (2014).

[4] A. Calcines, R. L. López, and M. Collados, "Musica: The multi-slit image slicer for the est spectrograph," *Journal of Astronomical Instrumentation* **2**(1) (2013).

[5] M. Landoni, M. Riva, P. Conconi, *et al.*, "Espresso apsu: simplify the life of the pupil slicing," *Proc SPIE* **8842** (2013).

[6] T. A. Birks, I. Gris-Sánchez, S. Yerolatsitis, *et al.*, "The photonic lantern," *Advances in Optics and Photonics* **7**(2), 107–167 (2015).

[7] E. Hubbard, J. Angel, and M. Gresham, "Operation of a long fused silica fiber as a link between telescope and spectrograph," *The Astrophysical Journal* **229**, 1074–1078 (1979).

[8] I. Parry, "The Astronomical Uses of Optical Fibers," in [*Fiber Optics in Astronomy III*], S. Arribas, E. Mediavilla, and F. Watson, eds., *Astronomical Society of the Pacific Conference Series* **152**, 3 (1998).

Downloaded From: https://www.spiedigitallibrary.org/conference-proceedings-of-spie on 17 Jan 2023
Terms of Use: https://www.spiedigitallibrary.org/terms-of-use

[9] J. M. Hill, J. R. P. Angel, J. S. Scott, *et al.*, "Multiple object spectroscopy - The Medusa spectrograph," *ApJ* **242**, L69–L72 (Dec. 1980).
[10] C. Vanderriest, "A fiber-optics dissector for spectroscopy of nebulosities around quasars and similar objects," *Publications of the Astronomical Society of the Pacific* **92**(550), 858 (1980).
[11] C. Vanderriest and J.-P. Lemonnier, "Silfid: A versatile fiber-optics spectrograph for faint objects," in [*Instrumentation for Ground-Based Optical Astronomy*], 304–310, Springer (1988).
[12] S. C. Barden and K. Scott, "The DensePak Fiber Array and Observations of NGC 7009," in [*Bulletin of the American Astronomical Society*], *baas* **18**, 951 (Sept. 1986).
[13] S. C. Barden and R. A. Wade, "Densepak and spectral imaging with fiber optics," in [*Fiber optics in astronomy*], **3**, 113–124 (1988).
[14] S. Arribas, E. Mediavilla, and J. Rasilla, "An optical fiber system to perform bidimensional spectroscopy," *The Astrophysical Journal* **369**, 260–270 (1991).
[15] M. Kimura, T. Maihara, F. Iwamuro, *et al.*, "Fibre multi-object spectrograph (fmos) for the subaru telescope," *Publications of the Astronomical Society of Japan* **62**(5), 1135–1147 (2010).
[16] G. J. Hill, P. J. MacQueen, L. W. Ramsey, *et al.*, "Performance of the hobby-eberly telescope and facility instruments," in [*Ground-based Instrumentation for Astronomy*], **5492**, 94–108, International Society for Optics and Photonics (2004).
[17] S. M. Croom, J. S. Lawrence, J. Bland-Hawthorn, *et al.*, "The sydney-aao multi-object integral field spectrograph," *MNRAS* **421**(1), 872–893 (2012).
[18] J. J. Bryant, J. Bland-Hawthorn, J. Lawrence, *et al.*, "Hector: a new massively multiplexed ifu instrument for the anglo-australian telescope," in [*Ground-based and Airborne Instrumentation for Astronomy VI*], **9908**, 99081F, International Society for Optics and Photonics (2016).
[19] S. Halverson, A. Roy, S. Mahadevan, *et al.*, "An efficient, compact, and versatile fiber double scrambler for high precision radial velocity instruments," *The Astrophysical Journal* **806**(1), 61 (2015).
[20] K. Strassmeier, I. Ilyin, A. Järvinen, *et al.*, "Pepsi: The high-resolution échelle spectrograph and polarimeter for the large binocular telescope," *Astronomische Nachrichten* **336**(4), 324–361 (2015).
[21] G. Courtes, "An integral field spectrograph (ifs) for large telescopes," in [*International Astronomical Union Colloquium*], **67**, 123–128, Cambridge University Press (1982).
[22] R. Bacon, G. Adam, A. Baranne, *et al.*, "3d spectrography at high spatial resolution. i. concept and realization of the integral field spectrograph tiger.," *Astronomy and Astrophysics Supplement Series* **113**, 347 (1995).
[23] J. Larkin, M. Barczys, A. Krabbe, *et al.*, "Osiris: a diffraction limited integral field spectrograph for keck," *New Astronomy Reviews* **50**(4-5), 362–364 (2006).
[24] R. U. Claudi, M. Turatto, R. G. Gratton, *et al.*, "SPHERE IFS: the spectro differential imager of the VLT for exoplanets search," in [*Ground-based and Airborne Instrumentation for Astronomy II*], *Proc SPIE* **7014**, 70143E (July 2008).
[25] J. K. Chilcote, J. E. Larkin, J. Maire, *et al.*, "Performance of the integral field spectrograph for the Gemini Planet Imager," in [*Ground-based and Airborne Instrumentation for Astronomy IV*], *Proc SPIE* **8446**, 84468W (Sept. 2012).
[26] M. A. Peters, T. Groff, N. J. Kasdin, *et al.*, "Conceptual design of the coronagraphic high angular resolution imaging spectrograph (charis) for the subaru telescope," in [*Ground-based and Airborne Instrumentation for Astronomy IV*], **8446**, 84467U, International Society for Optics and Photonics (2012).
[27] J. R. Allington-Smith, R. Content, R. Haynes, *et al.*, "Integral field spectroscopy with the gemini multiobject spectrographs," *Proc.SPIE* **2871**, 2871 – 2871 – 11 (1997).
[28] R. Haynes, D. Lee, J. Allington-Smith, *et al.*, "Multiple-object and integral field near-infrared spectroscopy using fibers," *Publications of the Astronomical Society of the Pacific* **111**(765), 1451 (1999).
[29] O. Le Fèvre, M. Saisse, D. Mancini, *et al.*, "Commissioning and performances of the VLT-VIMOS instrument," in [*Instrument Design and Performance for Optical/Infrared Ground-based Telescopes*], M. Iye and A. F. M. Moorwood, eds., *Proc. of SPIE* **4841**, 1670–1681 (Mar. 2003).
[30] M. M. Roth, A. Kelz, T. Fechner, *et al.*, "PMAS: The Potsdam Multi-Aperture Spectrophotometer. I. Design, Manufacture, and Performance," *PASP* **117**, 620–642 (June 2005).

Downloaded From: https://www.spiedigitallibrary.org/conference-proceedings-of-spie on 17 Jan 2023
Terms of Use: https://www.spiedigitallibrary.org/terms-of-use

[31] J. Schmoll, G. N. Dodsworth, R. Content, *et al.*, "Design and construction of the imacs-ifu: a 2000-element integral field unit," in [*Ground-based Instrumentation for Astronomy*], **5492**, 624–634, International Society for Optics and Photonics (2004).

[32] D. M. Haynes, M. J. Withford, J. M. Dawes, *et al.*, "Relative contributions of scattering, diffraction and modal diffusion to focal ratio degradation in optical fibres," *MNRAS* **414**, 253–263 (June 2011).

[33] D. Lee, R. Haynes, and D. Skeen, "Properties of optical fibres at cryogenic temperatures," *Monthly Notices of the Royal Astronomical Society* **326**(2), 774–780 (2001).

[34] I. S. Bowen, "The image-slicer a device for reducing loss of light at slit of stellar spectrograph," *Astrophysical Journal* **88**, 113 (1938).

[35] L. V. H. J. E. Simmons, Raleigh M. Drake, "Modified bowen-walraven image slicer," *Proc SPIE* **0331** (1982).

[36] F. Diego, "Toward total transmission: the confocal image slicer," *Proc SPIE* **2198** (1994).

[37] L. Weitzel, A. Krabbe, H. Kroker, *et al.*, "3D: The next generation near-infrared imaging spectrometer," in [*Astronomy and Astrophysics Supplement*], **119**, 531–546 (1996).

[38] M. Tecza, F. Eisenhauer, C. Iserlohe, *et al.*, "Spiffi image slicer: high-precision optics at cryogenic temperatures," *Proc SPIE* **4842** (2003).

[39] S. Eikenberry, R. Elston, R. Guzman, *et al.*, "Fisica: the florida image slicer for infrared cosmology and astrophysics," *Proc SPIE* **5492** (2004).

[40] S. S. Eikenberry, J. G. Bennett, B. Chinn, *et al.*, "Miradas for the gran telescopio canarias: system overview," *Proc SPIE* **8446**, 8446 – 8446 – 13 (2012).

[41] R. Content, "Optical design of the KMOS slicer system," in [*Proc SPIE*], **6269**, 6269–9 (2006).

[42] F. Laurent, E. Renault, R. Bacon, *et al.*, "Optical design, manufacturing, and tests of the muse image slicer," *Proc.SPIE* **5965**, 5965 – 5965 – 12 (2005).

[43] C. Bourgenot, D. J. Robertson, D. Stelter, *et al.*, "Towards freeform curved blazed gratings using diamond machining," in [*Proc SPIE*], **9912**, 99123M (2016).

[44] F. Laurent and F. Hénault, "Collimating slicer for optical integral field spectroscopy," in [*Proc SPIE*], **9912**, 99125R (2016).

[45] Y. Suematsu, K. Saito, M. Koyama, *et al.*, "Development of compact metal-mirror image slicer unit for optical telescope of the SOLAR-C mission," in [*Proc SPIE*], **9904**, 990411 (2016).

[46] P. Rees, R. Content, M. Dubbeldam, *et al.*, "Management of optical interfaces in the VLT KMOS instrument," in [*Modeling, Systems Engineering, and Project Management for Astronomy III*], *Proc SPIE* **7017**, 701707 (July 2008).

[47] S. Leon-Saval, T. Birks, J. Bland-Hawthorn, *et al.*, "Multimode fiber devices with single-mode performance," *Optics letters* **30**(19), 2545–2547 (2005).

[48] R. R. Thomson, T. A. Birks, S. Leon-Saval, *et al.*, "Ultrafast laser inscription of an integrated photonic lantern," *Optics express* **19**(6), 5698–5705 (2011).

[49] S. Yerolatsitis, K. Harrington, and T. A. Birks, "All-fibre pseudo-slit reformatters," *Opt. Express* **25**, 18713–18721 (Aug 2017).

[50] R. Thomson, R. Harris, T. Birks, *et al.*, "Ultrafast laser inscription of a 121-waveguide fan-out for astrophotonics," *Optics letters* **37**(12), 2331–2333 (2012).

[51] S. G. Leon-Saval, C. H. Betters, and J. Bland-Hawthorn, "The photonic tiger: a multicore fiber-fed spectrograph," in [*Proc. of SPIE Vol*], **8450**, 84501K–1 (2012).

[52] C. Q. Trinh, S. C. Ellis, J. Bland-Hawthorn, *et al.*, "Gnosis: the first instrument to use fiber bragg gratings for oh suppression," *The Astronomical Journal* **145**(2), 51 (2013).

[53] R. J. Harris, D. G. MacLachlan, D. Choudhury, *et al.*, "Photonic spatial reformatting of stellar light for diffraction-limited spectroscopy," *MNRAS* **450**(1), 428–434 (2015).

[54] A. Horton, S. Ellis, J. Lawrence, *et al.*, "Praxis: a low background nir spectrograph for fibre bragg grating oh suppression," in [*Modern Technologies in Space-and Ground-based Telescopes and Instrumentation II*], **8450**, 84501V, International Society for Optics and Photonics (2012).

[55] J. Bland-Hawthorn, S. Ellis, S. Leon-Saval, *et al.*, "A complex multi-notch astronomical filter to suppress the bright infrared sky," *Nature communications* **2**, 581 (2011).

Downloaded From: https://www.spiedigitallibrary.org/conference-proceedings-of-spie on 17 Jan 2023
Terms of Use: https://www.spiedigitallibrary.org/terms-of-use

[56] M. Corrigan, R. J. Harris, R. R. Thomson, *et al.*, "Wavefront sensing using a photonic lantern," in [*SPIE Astronomical Telescopes+ Instrumentation*], 990969–990969, International Society for Optics and Photonics (2016).
[57] R. Tamai and J. Spyromilio, "European extremely large telescope: progress report," *Proc SPIE* **9145** (2014).
[58] F. Zerbi and et al, "HIRES: the high resolution spectrograph for the E-ELT," in [*Proc SPIE*], **9147**, 914723 (2014).
[59] N. K. Fontaine, R. Ryf, J. Bland-Hawthorn, *et al.*, "Geometric requirements for photonic lanterns in space division multiplexing," *Opt. Express* **20**, 27123–27132 (Nov 2012).
[60] I. Gris-Snchez, D. M. Haynes, K. Ehrlich, *et al.*, "Multicore fibre photonic lanterns for precision radial velocity science," *Monthly Notices of the Royal Astronomical Society* **475**(3), 3065–3075 (2018).
[61] S. Van der walt, S. C. Colbert, and V. Gaël, "The NumPy array: a structure for efficient numerical computation," *Computing in Science & Engineering* **13**, 22–30 (2011).
[62] J. D. Hunter, "Matplotlib: A 2d graphics environment," *Computing In Science & Engineering* **9**(3), 90–95 (2007).

Downloaded From: https://www.spiedigitallibrary.org/conference-proceedings-of-spie on 17 Jan 2023
Terms of Use: https://www.spiedigitallibrary.org/terms-of-use